MOLECULAR PHYSICS, 1998, VOL. 95, NO. 6, 1325–1332

Multi-frequency EPR determination of zero field splitting of high spin species in liquids: Gd(III) chelates in water

R. B. CLARKSON[1,2], ALEX I. SMIRNOV[1], T. I. SMIRNOVA[3], H. KANG[1,3], R. L. BELFORD[1,3], K. EARLE[4], and JACK H. FREED[4]

Departments of [1]Medical Information Science, [2]Veterinary Clinical Medicine, [3]Chemistry, and the Illinois EPR Research Center, University of Illinois, Urbana, IL 61801, USA

[4]Department of Chemistry, Cornell University, Ithaca, NY 14853, USA

(*Received 25 April 1998; revised version accepted 8 July 1998*)

Multi-frequency EPR spectroscopy at 9.5, 35, 94, and 249 GHz has been employed to investigate the zero field splitting (ZFS) of high spin ions in liquids. In particular, experiments are reported on aqueous solutions of DTPA and DOTA chelates of Gd(III), and on the uncomplexed ion, which are relevant to the effectiveness of paramagnetic contrast agents for magnetic resonance imaging (MRI). The field dependence of the centroid of the resonance line, characterized by an effective g factor, $\mathbf{g}_{\text{eff}}$, has been analysed in order to determine Δ^2, the trace of the square of the ZFS matrix. Analysis of the variation in transverse electron spin relaxation (T_{2e}) with experimental frequency provides yet another route to measure Δ^2 from EPR data. This analysis also gives τ_v, a correlation time describing the time-dependent ZFS effect. The ZFS parameters so obtained agree well with results obtained by the analysis of proton nuclear magnetic relaxation dispersion. At 94 GHz, partially resolved spectra from chelated and unchelated Gd(III) were observed. The shifts in resonance field for Gd(III) in these two compounds are due primarily to differences in the magnitude of ZFS. The spectral resolution as a function of frequency exhibits a maximum in the range of our experiments; the resolution disappeared at either higher or lower resonance frequency. Study of ZFS by EPR at multiple high fields offers a new and sensitive route to probe water interactions and chelate dynamics in biologically relevant systems having high spin ions.

1. Introduction

As pointed out by Abragam and Bleaney [1], the ground state of the Gd(III) ion $(4f^7)$ is nearly pure $^8S_{7/2}$, with a slight admixture of $^6P_{7/2}$ through intermediate coupling. Perturbations from ligands cause a splitting of the electronic states, producing a fine structure in the resonance spectrum that can be represented by a simplified spin Hamiltonian of the form

$$\mathcal{H}_{\text{spin}} = \beta \mathbf{B} \cdot \mathbf{g} \cdot \boldsymbol{S} + \sum_{m,n} B_n^M O_n^m, \qquad (1)$$

where the second term describes the fine structure in terms of spin operators characterizing the effects of the ligand fields. While we may anticipate a number of higher-order terms for the $4f^7$ (ground state $s = 7/2$) ion, the very small orbital angular momentum in this system causes terms of higher degree to become rapidly smaller [1], and for this discussion they will be neglected. In single crystals, the expansion in $\{m,n\}$ often can be evaluated for specific ligand symmetries; in solutions, this term is less well defined, and generally is time dependent. Odelius, *et. al.* [2], discussing the analogous problem for Ni(II) $(3d^8, {}^3F_1)$, re-write the Hamiltonian as

$$\mathcal{H}_{\text{spin}} = \mathcal{H}_{\text{Zeeman}} + \mathcal{H}_{\text{ZFS}} = \beta \mathbf{B} \cdot \mathbf{g} \cdot \mathbf{S} + \mathbf{S} \cdot \mathbf{D}_{\text{ZFS}}(t) \cdot \mathbf{S}, \qquad (2)$$

where $\mathbf{D}_{\text{ZFS}}$ is the time dependent zero field splitting (ZFS) tensor, which describes the second-order coupling of the electron spins with the orbital angular momentum, and which removes some of the degeneracy in the spin states even in the absence of a magnetic field. For many years the time dependent fluctuations of the ZFS term have been thought to dominate electron spin relaxation in Gd(III) systems [3–8]. Prior workers have adopted a form of Bloch–Wangsness–Redfield (BWR) theory [9] to characterize the time dependent fluctuations of $\mathbf{D}_{\text{ZFS}}$ by means of an exponentially decaying correlation function, which defines a correlation time τ_v for the modulation of the ZFS. This approach requires that $\tau_v \ll T_{2e}$, a condition which Slichter characterizes as not asking for information over time intervals comparable with τ_v [9]. The inequality is not

strongly satisfied for Gd(III) chelates at 9.5 GHz, where τ_v/T_{2e} can approach 0.1, and it may be violated at lower frequencies. This point will be considered later in the discussion. Also it has been pointed out by several authors that when the ZFS term is large compared with the electronic Zeeman energy, a contribution to electron relaxation (and nuclear relaxation enhancement) can be expected from a *static* ZFS component [10, 11]. For many Gd(III) complexes, the magnitude of the ZFS is of the order of $0.1\,cm^{-1}$. At values of the magnetic field corresponding to X band EPR (0.34 T), the ZFS term is therefore less than the electronic Zeeman interaction, and its relative contribution to the Hamiltonian becomes proportionally smaller at higher fields. Since in our system $\mathcal{H}_{Zeeman} \gg \mathcal{H}_{ZFS}$ at the magnetic field values used in this study (the Zeeman limit), we interpret $\mathbf{D}_{ZFS}$ only in terms of the dynamic ZFS interaction.

The electron paramagnetic resonance (EPR) spectrum of a Gd(III) chelate in water is typically observed as a single resonance line whose *effective g* factor depends upon the experimental value of $\mathbf{B}_0$. Dynamic frequency shifts in EPR spectra were considered previously and treated using the Redfield relaxation matrix approach [12, 13]. Theoretical results were compared with experimental X and Q band EPR data. In another study, Smirnova *et al.* [14] calculated the frequency shift by averaging over all orientations the anisotropic shift derived from a static spin Hamiltonian. This treatment is based on the assumptions that molecular motion neither changes the spin precession rate nor perturbs the states and, thus, that the centre of gravity of the spectrum is invariant even in presence of motional averaging. For the allowed $|\frac{1}{2}\rangle \leftrightarrow \langle -\frac{1}{2}|$ transition under perturbation theory expressions valid up to the third order, this shift is given by [14]

$$\Delta_B = \frac{1}{20g\beta\omega_0}(4s(s+1)-3)(\tfrac{2}{3}D^2 + 2E^2). \qquad (3)$$

A more rigorous approach to analysing multifrequency EPR data would be to follow the treatment of Poupko *et al.* [13] which involves diagonalization of a *complex* relaxation matrix $\mathbf{R}$ and then simultaneously using the real part of eigenvalues for fitting the EPR line shapes and the imaginary part for analysing the apparent *g*-shift. This anaysis of the *g*-shift is especially important at X-band frequencies and lower where the static limit we are using begins to breaks down. This result is identical to the shift expression for spin 5/2 that Baram *et al.* [15] derived by using the semiclassical stochastic Liouville general formalism [16] in the limit when motional effects are negligible. For Gd(III) ion $(s = 7/2)$ the field shift (equation (4)) can be recast for an effective *g* factor, $\mathbf{g}_{eff}$, in terms of the squared ZFS matrix $\Delta^2 = D_{xx}^2 + D_{yy}^2 + D_{zz}^2$:

$$\mathbf{g}_{eff} = g\left(1 - \frac{3\Delta^2}{\omega_0^2}\right) = g\left(1 - \frac{3\Delta_f^2}{h^2\upsilon^2}\right), \qquad (4)$$

where υ is the resonance frequency; Δ is in units of radians/s^{-1}, while Δ_f is in units of Hertz (s^{-1}). Thus, the variation of $\mathbf{g}_{eff}$ with experimental frequency can be analysed to obtain Δ^2 [14].

Not only will the effective *g* factor shift with changes in the experimental frequency, the electron spin relaxation in Gd(III) chelates also will be strongly affected. Powell, *et al.* [8] give an excellent review of several approaches to interpreting the frequency dependence of T_{1e} and T_{2e} in these systems. We have adopted the approach of Hudson and Lewis [6], who showed that the eigenvalues ξ of the relaxation matrix $\mathbf{R}$ are functions of τ_v and the experimental frequency υ, and are related to the relaxation time T_{2ei} of the *i*th allowed electron spin transition by the expression

$$\frac{1}{T_{2ei}} = -\Delta^2\tau_v\xi. \qquad (5)$$

In their application of BWR theory, Hudson and Lewis assume that the dominant line-broadening mechanism is provided by the modulation of a second-rank tensor interaction (i.e., ZFS); higher-rank tensor contributions are assumed to be negligible. $\mathbf{R}$ is a 7×7 matrix for the $s = 7/2$ system, with matrix elements written in terms of the spectral densities $J(\omega, \tau_v)$ (see [6] and [9] for details). The intensity of the *i*th transition also can be calculated from the eigenvectors of $\mathbf{R}$. In general, there are four transitions with nonzero intensity at any frequency, raising the prospect of a multi-exponential decay of the transverse magnetization. There is not a one-to-one correspondence between the relaxation rates and the degenerate $|m_i\rangle \leftrightarrow |m_i \pm 1\rangle$ transitions, and one transition is predicted to have a T_{2ei} that is much longer than the other three. Figure 1 shows a plot of the eigenvalues (ξ) of the four nonzero transitions as a function of frequency. Particularly at frequencies greater than 35 GHz, the differences between the longest T_{2ei} and the other three values are predicted to be greater than a factor of 10, which suggests that in continuous wave EPR experiments the spectrum of Gd(III) will consist of a narrow line superimposed on very much broader, weaker lines. The narrow line shape is likely to dominate any fitting of the spectrum by Lorentzian functions in an analysis to determine approximate values of T_{2e}, a prediction that we found borne out by our experiments. A multi-frequency study of Gd(III) chelates in solution thus also yields information about the ZFS through changes in T_{2e} with frequency.

2. Experimental

Three different Gd(III) complexes were studied. The compounds were complexes of diethylenetriaminepen-

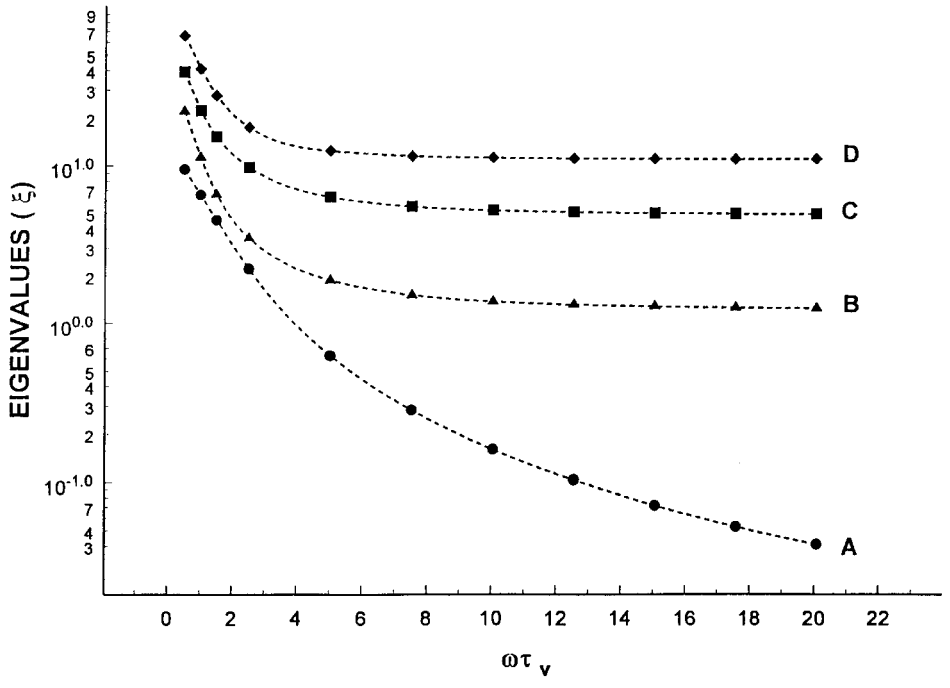

Figure 1. Frequency variation of the eigenvalues ξ of the four spin transitions with nonzero intensity (A–D) for an $s = 7/2$ system, as calculated by the method of Hudson and Lewis [6]. The ξ are directly related to predicted values of T_{2e}

taacetic acid (DTPA), and of 1,4,7,10-tetraazacyclododecane-*N*,*N*,*N*,*N*-tetraacetic acid (DOTA); all were synthesized by Schering, AG, Berlin, and used as received without further purification. Solutions were prepared with triply distilled deionized water. Concentrations were adjusted to be 1.0 mM for DTPA and DOTA complexes. The concentration of $GdCl_3$ (Aldrich, Milwaukee, WI) was 3 mM.

X band and Q band measurements were made utilizing commercial Varian E-line spectrometers. W band measurements were made on a locally built instrument operating at a nominal frequency of 94 GHz [17]. The 249 GHz experiments were performed on an instrument built at Cornell University [18]. All measurements were made at room temperature. Magnetic field strengths were calibrated with a PT 2025 Metralab precision NMR teslameter (GMW Associates, Redwood City, CA), and experimental frequencies were measured with an EIP 578 digital frequency counter (EIP Microwave, Inc., San Jose, CA).

EPR line positions and apparent Lorentzian linewidths were obtained from the digital experimental data utilizing numerical methods developed by Smirnov and Belford [19]. Numerical evaluation and diagonalization of the relaxation matrix **R** employed Mathcad 6.0 (Mathsoft, Inc, Cambridge, MA).

3. Results

Figure 2 illustrates EPR spectra of Gd(III) DTPA aqueous solutions at experimental frequencies of 9.5,

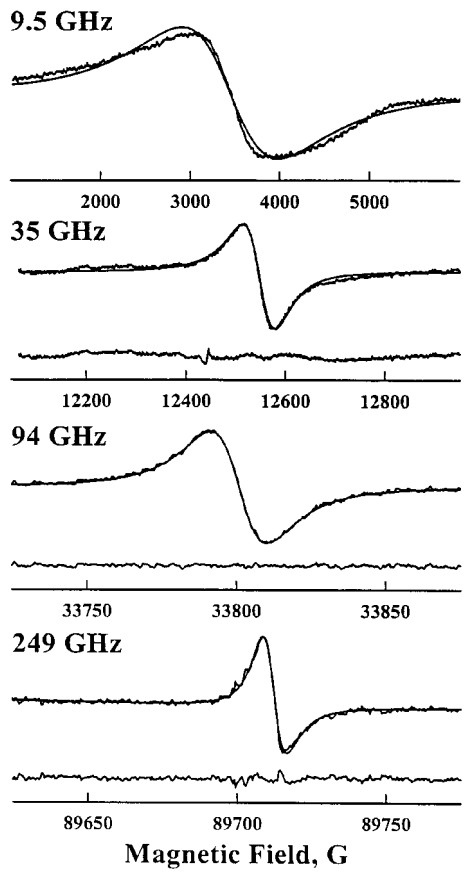

Figure 2. EPR spectra of a 1.0 mM aqueous solution of Gd-DTPA, measured at 9.5, 35, 94, and 249 GHz. The solid lines are best Lorentzian fits to the data. The trace at bottom of graphs is residual.

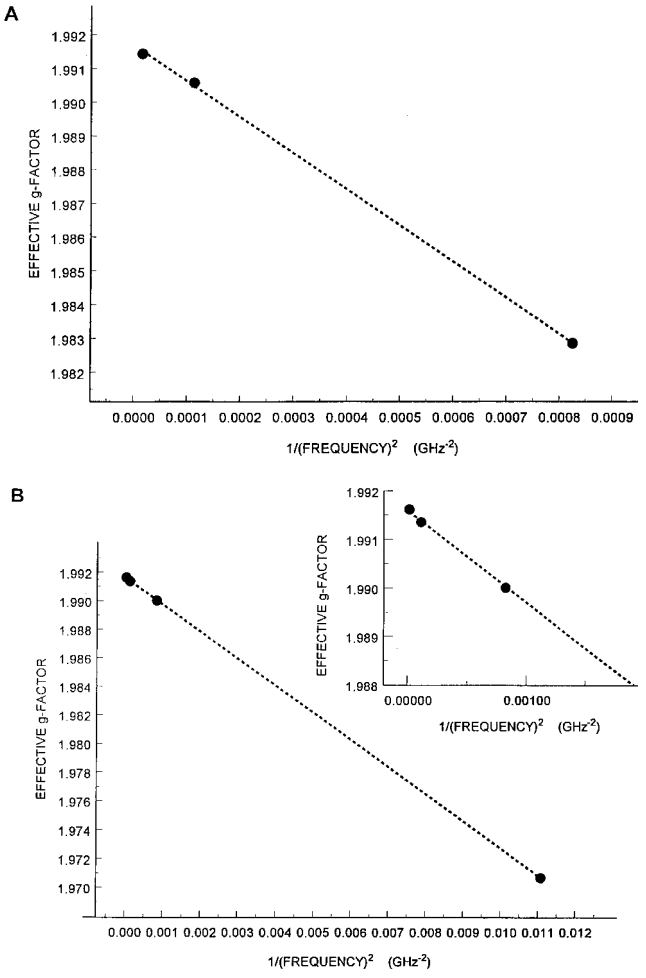

Figure 3. The variation of $\mathbf{g}_{\mathrm{eff}}$ as a function of the inverse square of the experimental frequency. The slopes of the best straight lines through the data are used to calculate Δ^2 according to equation (4). (*a*) Gd-DTPA, 1.0 mM aqueous solution, $\Delta^2 = 7 \times 10^{19}$ rad^2 s^{-2}; (*b*) Gd-DOTA, 1.0 mM aqueous solution, $\Delta^2 = 1.24 \times 10^{19}$ rad^2 s^{-2}.

Table 1. Multi-frequency EPR parameters for Gd(III) chelates in water at 22 °C.

Experimental frequency/GHz	Gd-DTPA, 1.0 mM		Gd-DOTA, 1.0 mM	
	$\mathbf{g}_{\mathrm{eff}}$	$\Delta B_{\mathrm{pp}}/G$	$\mathbf{g}_{\mathrm{eff}}$	$\Delta B_{\mathrm{pp}}/G$
9.5	N/A	620	1.9705(5)	81
34.8	1.9828(5)	63.8	1.9900(0)	25.9
94.1	1.9905(7)	19.1	1.9913(5)	13.6
249	1.9914(3)	7.8	1.9916(1)	5.8

35, 94, and 249 GHz. Table 1 summarizes the peak-to-peak linewidths and *effective g* factors for this complex and for Gd(III) DOTA. Figure 3 (*a*,*b*) shows the variation of $\mathbf{g}_{\mathrm{eff}}$ as a function of the inverse square of the

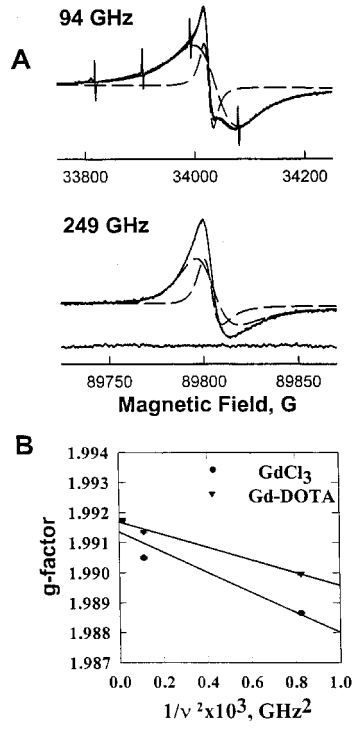

Figure 4. (*a*) 94 GHz and 249 GHz EPR spectra of $GdCl_3$/Gd-DOTA aqueous solution. Beneath each spectrum is a least-squares fit of the data, using a simple two-Lorentzian model. Adjustable phase shift was included in the simulation. The magnetic field separation between line centres is 14 G at 94 GHz, and 5.8 G at 248 GHz. Sharp lines superimposed on the 94 GHz EPR spectrum are from $Mn^{2}+$ used as a field marker. (*b*) Variation of $\mathbf{g}_{\mathrm{eff}}$ with the inverse square of the experimental frequency for $GdCl_3$ and Gd-DOTA signals. The best straight lines through the data points allowed the calculation of Δ^2 for the $GdCl_3$: $\Delta^2 = 2.2 \times 10^{19}$ rad^2 s^{-2}; for Gd-DOTA: $\Delta^2 = 1.2 \times 10^{19}$ rad^2/s^2.

experimental frequency for the two complexes. The good linearity of the plots lets us determine Δ^2 in each system (equation (5)): 7.0×10^{19} for rad^2 s^{-2} Gd DTPA and $1.2(4) \times 10^{19}$ rad^2 s^{-2} for Gd-DOTA. Similar values for the ZFS have been obtained by other methods for other aqueous Gd(III) complexes [8, 20–23].

When unchelated Gd(III) was present in a solution together with chelated Gd(III) (Gd-DOTA), a partial splitting was observed in the 94 GHz EPR spectrum (figure 4). The splitting disappeared at 35 GHz or 249 GHz. Similar splittings in HF EPR spectra were observed when a lipophilic derivative of DOTA containing an n-pentane side chain, DOTA-P, partitioned between aqueous and lipid phases of multilamellar DMPC liposomes [14]. The EPR spectra of this system at 94 GHz and 249 GHz exhibit two resonance lines, corresponding to signals from the aqueous and lipid environments. Similar, but less well resolved spectra,

are observed when lipophilic chelates, such as DOTA-P and the ethoxybenzoate derivative of DTPA, DTPA-EOB, interact with human serum albumin and with hepatocytes [24]. We attribute the splitting at 94 GHz from the $GdCl_3$/Gd-DOTA solution to the effect of chelating on the ZFS. The *effective g* factors for signals arising from the unchelated Gd(III), which has a broader line, and Gd-DOTA plotted as functions of the inverse square of the experimental frequency, are shown in figure 4(*b*). The slopes of the plots of $\mathbf{g}_{\mathrm{eff}}$ as a function of υ^{-2} in the two environments are observed to be different, leading to the conclusion that Δ^2 is different for chelated and unchelated Gd(III). For $GdCl_3$, Δ^2 is found to be 2.2×10^{19} rad^2 s^{-2} and for Gd-DOTA, 1.2×10^{19} rad^2 s^{-2}. Figure 4(*a*) also shows that when this system is observed at two different spectrometer frequencies, 94 GHz and 249 GHz, the absolute magnetic field separation of the two resonances is greater at 94 GHz than it is at 249 GHz, again leading to the conclusion that it is the field independent ZFS term that is the major cause of $\mathbf{g}_{\mathrm{eff}}$ difference in these two resonances.

The spectra of Gd-DTPA at different microwave frequencies shown in figure 2 are accompanied in each case by the best-fit Lorentzian lineshape. While the spectrum at X band is only approximately Lorentzian, the spectra at higher frequencies are well fitted by the Lorentzian function. This fact can be used to calculate the approximate values of T_{2e} for each frequency, according to the relationship $1/T_{2e} = \Delta B_{pp}\gamma\frac{\sqrt{3}}{2}$, where ΔB_{pp} is the peak-to-peak linewidth of the first-derivative spectrum.

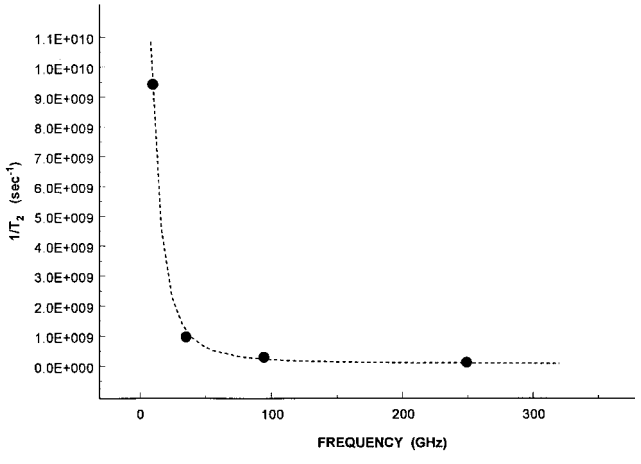

Figure 5. Variation of calculated values of $1/T_{2e}$ with experimental frequency for Gd-DTPA in aqueous solution. Superimposed on the data is the bet fit using the relaxation matrix given by Lewis and Hudson [6], calculating the narrowest line at each frequency (dotted line). The approach is patterned after the work of Reuben [7]. Best fit values are: $\Delta^2 = 8 \times 10^{19}$ rad^2 s^{-2}, $\tau_v = 2.4 \times 10^{-11}$ s, and $R_0 = 7.6 \times 10^6$ s^{-1}.

Results are shown in figure 5 for Gd-DTPA. The frequency behaviour observed was accounted for by the approach of Reuben [7], i.e., one of the four nonzero rates will be significantly slower than the others, contributing a narrower linewidth which will dominate the observed peak-to-peak EPR line width. At all four spectrometer frequencies we report here, this assumption is validated by the results calculated from **R** (equation (6)), which indicate that in each case one transition does have a transverse relaxation rate much slower than the other three (figure 1). Consequently, values of T_{2ei} were calculated for each of the four experimental frequencies, and only the longest relaxation time was used in each instance. The experimental data were fitted by allowing the values of Δ^2 and τ_v to vary, making use of a non-linear least squares procedure, and calculating eigenvalues of the **R** matrix at each τ_v value. A field independent relaxation rate, R_0, also was added to the fitting equation, which then became

$$\frac{1}{T_{2e}} = \frac{1}{T_{2ei}(\omega)} + R_0. \qquad (6)$$

A field independent contribution to the transverse relaxation rate has been observed by others [25, 26], although the exact mechanism(s) responsible for R_0 is still the subject of investigation. Figure 5 shows that this model accounts very well for the frequency dependence of T_{2e} in the Gd-DTPA system. A similar agreement between experiment and calculation was obtained on data from Gd-DOTA. Since the calculation of the T_{2ei}'s can be expressed as functions of Δ^2 and τ_v as shown in equation (6), the fitting of transverse relaxation dispersion data also provides another route to estimating the ZFS interaction parameters. Table 2 summarizes the results for ZFS parameters obtained by fitting the frequency dependence of $\mathbf{g}_{\mathrm{eff}}$ and T_{2e},

Table 2. ZFS analysis of Gd(III) chelates (1.0 mM aqueous solutions at 22 °C).

Gd(III) complex	Δ/rad^2 s^{-2}	τ_v/s
Gd-DTPA		
NMRD analysis [21]	5.3×10^{19}	1.9×10^{-11}
$\mathbf{g}_{\mathrm{eff}}$ vs B_0	7.0×10^{19}	N/A
$1/T_{2e}$ vs B_0[a]	8×10^{19}	2.4×10^{-11}
Powell *et al.* [23]	4.6×10^{19}	2.5×10^{-11}
Gd-DOTA		
NMRD analysis [20]	7×10^{18}	2.6×10^{-11}
$\mathbf{g}_{\mathrm{eff}}$	1.24×10^{19}	N/A
$1/T_{2e}$ vs B_0[a]	1.1×10^{19}	1.26×10^{-11}
Powell *et al.* [23]	1.6×10^{19}	1.1×10^{-11}

[a] Fitted by equation (6), in which $R_0 = 7.6 \times 10^7$ s^{-1} for Gd-DTPA and Gd-DOTA.

plus results from a Solomon–Bloembergen–Morgan analysis of proton nuclear magnetic relaxation dispersion (T_{1p} nuclear magnetic relaxation dispersion (NMRD)) data [20, 21].

4. Discussion

Multi-frequency EPR spectroscopy can provide useful information on the ZFS in Gd(III) chelates. Previous calculations of the Δ^2 and τ_v terms for these molecules in aqueous solution relied on an analysis of proton NMRD data, making use of inner-sphere point-dipole models (Solomon–Bloembergen–Morgan theory), which incorporate frequency dependent terms to calculate the electron spin relaxation rates as they are reflected in proton relaxation enhancement by the paramagnetic species [20, 21, 23, 27, 28]. Such analyses necessarily require the optimization of multi-parameter models, and the uniqueness of the best fits of theory with experiment is always a matter of concern. Recently, ^{17}O NMR relaxation in aqueous solutions of Gd(III) chelates has been studied in variable temperature, pressure, and magnetic field experiments, and ZFS values were extracted by analysis of the data [25]. Similar variable temperature and variable magnetic field EPR experiments also have been performed, from which ZFS parameters were obtained [8, 29]. In a recent summary of their work incorporating ^{17}O NMR, variable field, temperature, and pressure EPR, and NMRD techniques, Merbach and coworkers [23] give values for the important parameters that characterize several Gd(III) monomer and dimer chelates. Their values for Δ^2 and τ_v in Gd-DTPA and Gd-DOTA (aqueous solutions) are listed in table 2. The experiments reported in this paper employ only variable field/frequency EPR, making direct use of the magnetic field dependence of the spin Hamiltonian and the relaxation matrix, thus avoiding the complexity of analysing electron relaxation from its effects on nuclear relaxation. Our approach also avoids the necessity of performing variable temperature measurements and of considering the effects of temperature on spin relaxation and water exchange rates, which can be particularly complex in biological systems involving living cells or tissues. Results from previous work agree well with the values of Δ^2 and τ_v obtained here from the analysis of the field dependence of $\mathbf{g}_{eff}$, and transverse relaxation (T_{2e}) dispersion (electron magnetic relaxation dispersion, (EMRD).

The approximations used in calculating ZFS values from the analysis of transverse relaxation dispersion data should be mentioned as potential sources of error. It is important to keep in mind that the relaxation model employed here makes use of the general Bloch–Wangsness–Redfield approach [9]. This approach assumes that $\tau_v \ll T_{2e}$, an inequality that is not strongly satisfied for Gd(III) chelates observed at frequencies of 9.5 GHz and below. Therefore, to make better use of EMRD as a method for examining ZFS interactions in these systems, it would be preferable if experimental frequencies were chosen in the range 15 GHz and higher, although the Δ^2 values calculated from EMRD data including the 9.5 GHz observation are almost identical to those values derived from $\mathbf{g}_{eff}$ dispersion measurements. It also should be noted that the EPR lineshapes of Gd(III) complexes in solution at 9.5 GHz are not strictly Lorentzian functions, and therefore the estimation of T_{2e} from ΔB_{pp} might not be as accurate at this frequency. The origin of the complex lineshapes at lower EPR frequencies, especially for Gd DTPA, warrants further study. In fact, better methods are needed to relate EPR lineshapes and T_{2e} at any frequency, since the single spectral line observed from Gd(III) chelate solutions is a composite of four nonzero transitions with different transverse relaxation rates and different intensities, and also may contain contributions from forbidden spin transitions, particularly at lower experimental frequencies. Finally, currently it is unclear if any of the Gd complexes exhibit a g anisotropy sufficient to contribute to the linewidths observed in solution at high EPR frequencies.

In order to account for our observed relaxation rate data, we found it necessary to include an empirical field-independent term R_0 in the rate equation (equation 7). The value of R_0 was the same for both complexes, $7.6 \times 10^7\ s^{-1}$. Concentrations of Gd in our experiments were low enough to exclude spin–spin broadening as an important relaxation mechanism (see [23] for a discussion of concentration dependent linewidths at 5.0 T). In a ^{17}O NMR relaxation study, González, *et al.* [25] also found a field independent process of the same magnitude. While several suggestions have been forwarded as mechanisms for this additional relaxation (e.g., spin–rotation, non-dispersive contribution from ZFS modulation [26]), the exact nature of the process is still under investigation.

The resolution of spectra from chelated and unchelated Gd(III) demonstrated here or Gd-DOTA-P partitioned between aqueous and lipid phases reported in [14] is seen to be due largely to differences in the ZFS parameters for the complex in the two microenvironments. The best EPR resolution of signals from Gd(III) in two environments is obtained at a spectrometer frequency which depends upon Δ^2 at each site and the relationship between B_0 and the linewidth. In this study, spectra from chelated and unchelated Gd(III) show two signals which are better resolved at 94 GHz than at 249 GHz (figure 3(*a*)). To make an approximate model for the frequency dependence of

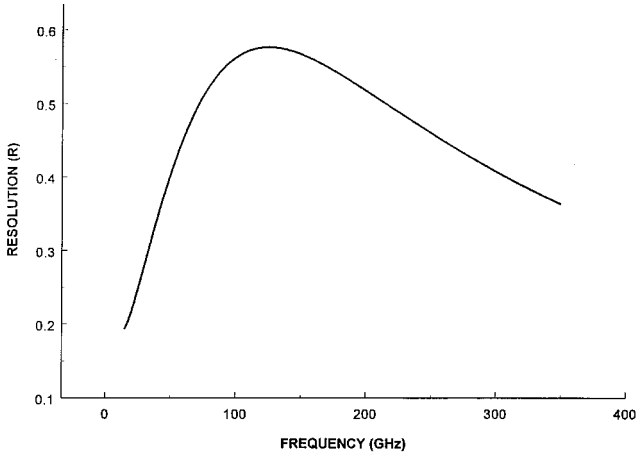

Figure 6. Variation of the spectral resolution R with the spectrometer frequency. In the simulation, $\Delta^2(1) = 3 \times 10^{19}$ rad^2 s^{-2}, $\Delta^2(2) = 2 \times 10^{20}$ rad^2 s^{-2}, and τ_v for both compoments is 2×10^{-11} s

spectral resolution, we adopt a simple definition of resolution:

$$\text{Resolution} = \frac{[B_0(1) - B_0(2)]}{\langle \Delta B_{pp} \rangle_{av}} \qquad (7)$$

Here, $B_0(1,2)$ are the line centres of the two signals, calculated from equation (4), and $\langle \Delta B_{pp} \rangle_{av}$ is the average linewidth of the individual signals. If the line shapes are Lorentzian, and if Reuben's relationship [7] between T_{2e} and B_0 is used to calculate ΔB_{pp} as a function of spectrometer frequency/field, then figure 6 illustrates how resolution varies with experimental frequency for a system in which $\Delta^2(1) = 3 \times 10^{19}$ rad^2 s^{-2}, $\Delta^2(2) = 2 \times 10^{20}$ rad^2 s^{-2}, and τ_v for both components is 2×10^{-11} s. The frequency at which maximum resolution is achieved will depend upon the difference in Δ^2 between the two sites and the exact form of line shape sensitivity to experimental frequency, but the general shape of the curve given in figure 6 agrees with the experimental data.

Environmental effects on Δ^2 and τ_v may reflect a sensitivity of the ZFS to (1) differences in the interactions with water in aqueous and lipid phases, and (2) differences in chelate dynamics in phases with different viscosities and dielectric constants. Koenig has speculated on the differences of water dynamics in lipid and aqueous phases [30], pointing out how much more 'dilute' water is in a lipid environment owing to low solubility, and Odelius *et al.* [2] and Kowall *et al.* [31] have made molecular dynamics calculations to show how water in the inner hydration sphere of $S > 1/2$ paramagnetic metal ions leads to observed ZFS effects. It will be important to investigate the sensitivity of the ZFS to water and chelate dynamics, and experiments now in progress will address these questions. Since Gd(III) chelates are being developed and applied as paramagnetic contrast agents in magnetic resonance imaging (MRI), this variation in the ZFS parameters with environment may be important in understanding the proton relaxation enhancement effects of these compounds in various biological systems, which often contain aqueous and lipid compartments.

An analysis of the magnetic field dependence of the spin Hamiltonian and the relaxation matrix for several Gd(III) chelates in aqueous solutions has demonstrated that the ZFS parameters Δ^2 and τ_v can be obtained from these data. The method avoids the difficulties posed by other methods that previously have been used to analyse the ZFS effects for metal ions in solution. In spite of the approximations in this investigation, the values of ZFS parameters for the Gd(III) chelates in aqueous solution reported here are in good agreement with other results in the literature. The simple, direct variable field/frequency EPR methods presented in this paper thus constitute a useful new approach, and further development of the method is warranted.

Partial support for this work was provided through grants from the National Institutes of Health (R01-GM42208, R.B.C; P41-RR01811, R.L.B; R01-GM25862 and R01-RR07216, J.H.F; F32-CA73156, T.I.S.). Contents of this report are solely the responsibility of the authors and do not necessarily represent official views of the National Cancer Institute, National Institute of General Medical Sciences, or National Center for Research Resources. Some facilities were provided by the Illinois EPR Research Center, an NIH-funded Resource Center. Gd(III) complexes were provided by Dr. B. Radüchel and colleagues, Schering, AG, Berlin, Germany. Professor Peter Petillo, University of Illinois at Urbana/Champaign, is thanked for valuable discussions.

References

[1] Abragam, A., and Bleaney, 1970, *Electron Paramagnetic Resonance of Transition Ions* (Oxford University Press) p. 335.
[2] Odelius, M., Ribbing, C., and Kowalewski, J., 1996, *J. chem. Phys.*, **104,** 3181.
[3] Bloembergen, N., and Morgan L. O., 1961, *J. chem. Phys.*, **34,** 842.
[4] McLachlan, A. D., 1964, *Proc. R. Soc. Lond.* A, **280,** 271.
[5] Hudson, A., and Luckhurst, G. R., 1969, *Molec. Phys.*, **16,** 395.
[6] Hudson, A., and Lewis, J. W. E., 1970, *Trans. Faraday Soc.*, **66,** 1297.
[7] Reuben, J., 1971, *J. phys. Chem.*, **75,** 3164.
[8] Powell, D. H., Merbach, A. E., Gonzàlez, G., Brücher, E., Micskei, K., Ottaviani, M. F., Köhler,

K., von Zelewsky, A., Grinberg, Ya. O., and Lebedev, Ya. S., 1993, *Helv. Chim. Acta*, **76,** 2129.
[9] Slichter, C. P., *Principles of Magnetic Resonance*, 1993, (Berlin: Springer-Verlag) p. 167.
[10] Sharp, R. R., 1993, *J. chem. Phys.*, **98,** 2507.
[11] Bertini, I., Galas, O., Luchinat, C., and Parigi, G., 1995, *J. magn. Reson* A, **113,** 151.
[12] Fraenkel, G. K., 1965, *J. chem. Phys.*, **42,** 4275.
[13] Poupko, R., Baram, A., and Luz, Z., *Molec. Phys.*, **27,** 1345.
[14] Smirnova, T. I., Smirnov, A. I., Belford, R. L., and Clarkson, R. B., 1998, *J. Amer. chem. Soc.*, **120,** 5060.
[15] Baram, A., Luz, A., and Alexander, S., 1973, *J. chem. Phys.*, **58,** 4558.
[16] Freed, J. H., Bruno, G. V., and Polnaszek, C. F., 1971, *J. phys. Chem.*, **75,** 3386.
[17] Wang, W., Belford, R. L., Clarkson, R. B., Davis, P. H., Forrer, J., Nilges, M. J., Timken, M. D., Walczak, T., Thurnauer, M. C., Norris, J. R., Morris, A. L., and Zhang, Y., 1994, *Appl. magn. Reson.*, **6,** 195.
[18] Lynch, W. B., Earle, K. A., and Freed, J. H., 1988, *Rev. sci. Instrum.*, **59,** 1345.
[19] Smirnov, A. I., and Belford, R. L., 1995, *J. magn. Reson.* A, **113,** 67.
[20] Aime, S., Anelli, P. L., Botta, M., Fedeli, F., Grandi, M., Paoli, P., and Uggeri, F., 1992, *Inorg. Chem.*, **31,** 2422.
[21] Uggeri, F., Aime, S., Anelli, P. L., Botta, M., Brocchetta, M., de Haën C., Ermondi, G., Grandi, M., and Paoli, P., 1995, *Inorg. Chem.*, **34,** 633.
[22] Geraldes, C. F. G. C., Urbano, A. M., Alpoim, M. C., Sherry, A. D., Kuan, K.-T., Rajagopalan, R., Maton, F., and Muller, R. N., 1995, *Magn. Reson. Imaging.*, **13,** 401.
[23] Powell, D. H., Ni Dhubhghaill, O. M., Pubanz, D., Helm, L., Lebedev. Ya. S., Schlaepfer, W., and Merbach, A. E., *J. Amer. chem. Soc.*, **118,** 9333.
[24] Smirnova, T. I., Smirnov, A. I., Belford, R. L., and Clarkson, R. B., 1996, Abstract, International Society for Magnetic Resonance in Medicine, 4th Scientific Meeting, New York.
[25] González, G., Powell, D. H., Tissières, V., and Merback, A. E., 1994, *J. phys. Chem.*, **98,** 53.
[26] Banci, L., Bertini, I., and Luchinat, C., 1991, *Nuclear and Electron Relaxation: The Magnetic Nucleus-Unpaired Electron Coupling in Solution* (New York: VCH).
[27] Chen, J. W., Auteri, F. P., Budil, D. E., Belford, R. L., and Clarkson, R. B., 1994, *J. phys. Chem.*, **98,** 13 452.
[28] Koenig, S. H., and Epstein, M., 1975, *J. chem. Phys.*, **63,** 2279.
[29] Powell, D. H., González, G., Tissières, V., Micskei, K., Brücher, E., Helm, L., and Merchbach, A. E., 1994, *J. Alloys Compds*, **207/208,** 20.
[30] Koenig, S. H., 1995, *Encyclopedia of NMR*, edited by Sunney I. Chan (Chichester: Wiley) p. 1819.
[31] Kowall, Th., Foglia, F., Helm, L., Merbach, A. E., 1995, *J. phys. Chem.*, **99,** 13 078.